

Report on Proposed Program of Research

Search for Physics Beyond the Standard Model with Vector Boson Scattering at the ATLAS Experiment

Nadia Davidson

Supervisor: Dr Elisabetta Barberio

Experimental Particle Physics Group

School of Physics



The University of Melbourne

March 25, 2007

Table of Contents

1	Summary of Proposed Research	2
2	Theoretical Motivation	3
2.1	The Standard Model	3
2.2	Physics Beyond the Standard Model at the TeV scale	4
2.3	Vector Boson Scattering (VBS) in the Absence of a Low Mass Higgs	5
3	Experiment	6
3.1	ATLAS and the LHC	6
3.2	VBS Resonance Detection	7
3.3	Calibration with Minimum Bias Events	7
4	Progress to Date	11
4.1	VBS Analysis	11
4.2	Calibration with Minimum Bias Events	11
5	List of Publications and Presentations	15
5.1	ATLAS Internal Notes	15
5.2	Presentations External to the University of Melbourne	15
6	Proposed Schedule and Timeline	17
6.1	Timeline to date	17
6.2	Timeline of proposed research	18

Chapter 1: Summary of Proposed Research

Although predictions from the Standard Model (SM) of particle physics has been in astonishing agreement with precision measurements of electroweak interactions, the mechanism of electroweak symmetry breaking (EWSM) is not yet known. The SM predicts a scalar potential with a non-zero vacuum expectation value which spontaneously breaks electroweak symmetry, giving mass to the W and Z gauge bosons. It is hoped that the scalar boson associated with this mechanism, the Higgs boson, will be discovered with the Large Hadron Collider (LHC) when 14TeV proton-proton collisions begin in 2008. Two general purpose detectors ATLAS and CMS are being built for the LHC and will be capable of observing the Higgs in the favoured mass range, 114 GeV - 186 GeV[1]. However, if the Higgs is not found in the mass region below 1 TeV as expected the mechanism for EWSB maybe studied via vector boson scattering. High mass resonances in the WZ and WW channels are predicted by a number of Beyond Standard Model theories in which dynamical EWSB occurs. The goal of my research will be to examine the extent to which the ATLAS detector at the LHC can measure or limit the existence of high mass vector-boson pair resonances.

Particular attention will be played to the role of jets in these events. As the dominant W and Z decays are into quarks, jets play an important role in the reconstruction of the resonant mass. Any measurement of jet energy will be restricted by the accuracy of the absolute jet energy scale. Thus, part of this research will be a calibration study. Specifically, the calibration of the single hadrons energy scale with use of the E/p method. This is a method in which the accurate measurement of momentum, p , from the inner tracker will be transferred to energy deposits in the calorimeters, E . This will be done using isolated pions from minimum bias (soft interactions).

Another application of minimum bias events is the calibration of transverse missing energy, E_T^{miss} . The resolution of this quantity will be studied. A good measurement of E_T^{miss} is needed for any mass reconstruction involving final state neutrinos. For example, in vector boson scattering this includes channels in which a W or Z decay into neutrinos. Additionally, many Beyond Standard Model theories such as supersymmetry predict the existence of new heavy weakly interacting particles which could potentially be produced at the LHC. In such situations, a signature of the new physics is large E_T^{miss} . Distinguishing this from background would require an understanding of any detector effects which lead to fake high E_T^{miss} in SM events.

Thus, there are two distinct areas of study proposed. The later of these has the potential to influence the outcome of the former.

- A physics analysis for vector boson scattering in the absence of a low mass Higgs.
- A study of calibration using minimum bias events with an aim to contribute to the precision of measurements with the ATLAS calorimeters.

Chapter 2: Theoretical Motivation

2.1 The Standard Model

The Standard Model of particle physics is the currently accepted theory which describes all known fundamental particles and their interactions. Particles can be broken up into two groups: fermions with half integer spin and bosons with integer spin. The fermions (quarks and leptons) make up regular matter while the bosons (the W , Z , γ and g) are force carriers. Figure 2.1 summarises the interaction between these particles.

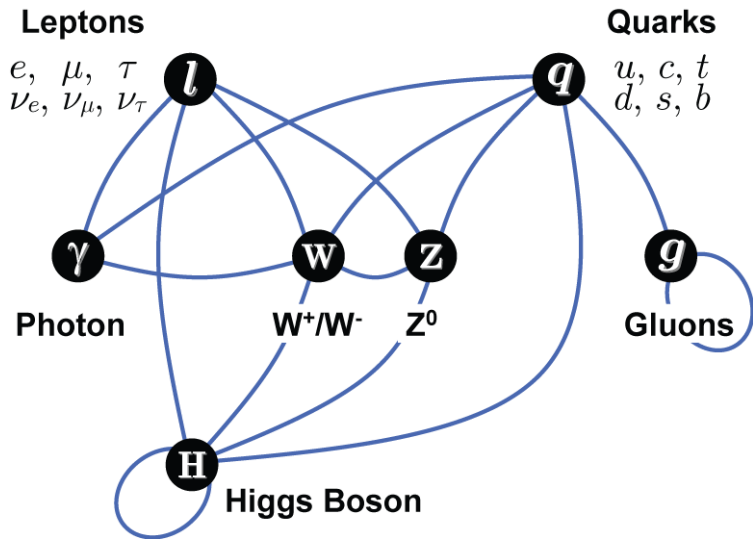


Figure 2.1: Interactions in the Standard Model[7]

The Standard Model belongs to the gauge group $SU(3)_C \otimes SU(2)_L \otimes U(1)_Y$. The $SU(3)_C$ gauge invariance of the Standard Model Lagrangian describes the strong force and $SU(2)_L \otimes U(1)_Y$ electroweak. $SU(2)_L \otimes U(1)_Y$ gauge invariance is spontaneously broken in the vacuum by a Higgs field doublet. The gauge bosons and fermions acquire a mass through interacting with this field. Three components of the Higgs field become the longitudinal third-polarisation components of the massive W and Z bosons.

The other component corresponds to a massive neutral boson; the Higgs boson. While the vacuum expectation value of the Higgs field is required to be 247 GeV [1] due to coupling with fermions, the Higgs boson mass is not predicted by the Standard Model. However, precision electroweak observables are sensitive to the Higgs mass through radiative corrections. They can constrain it to lie below 186 GeV (at 95% confidence level) [9]. Direct searches give a lower bound of 114.4 GeV[9].

2.2 Physics Beyond the Standard Model at the TeV scale

There is cause to believe that the Standard Model is not a complete theory but an low energy effective field theory. A number of deficits in the SM have inspired the search for new theories. These include:

1. The Higgs has not yet been observed, so variation from the SM EWSB mechanism are possible.
2. The Higgs bare mass must be finely tuned to give an observed mass in the favoured range. This is due to quadratically diverging quantum radiative correction to the mass of any scalar particles within the SM.
3. The SM does not include gravity.
4. There is no explanation for dark matter or dark energy.
5. There is no mechanism for neutrino oscillations.

One consequence of 2. from above is the dependence of the maximum Higgs mass on the scale of new physics, Λ . As shown in Figure 2.2, the Higg mass is confined to be below the 1 TeV mass region in order to preserve unitarity. This means new physics could potentially be seen at the LHC if the Higgs boson is heavier than expected. Even if a low mass Higgs is seen, resolutions of the fine-tuning problem, such as in supersymmetry and extra dimensions, would imply new physics at the TeV scale.

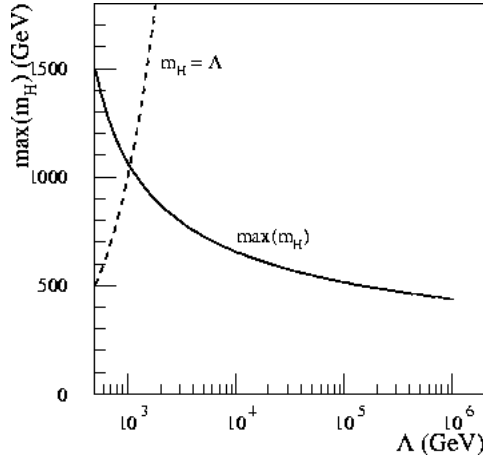


Figure 2.2: Dependence of Higgs Mass on New Physics

2.3 Vector Boson Scattering (VBS) in the Absence of a Low Mass Higgs

In the case that a Higgs boson (SM or otherwise) is not seen in the low mass range we would expect strong EWSB. Longitudinal Vector Boson Scattering (VBS) will play an important role in examining the mechanism of EWSB. This is because, as mentioned in section 2.1, three components of the Higgs field become the longitudinal components of the gauge bosons. The mass of the Higgs is related to the strength of the vector boson coupling.

Several theories allow for strongly coupled dynamical EWSB, for example composite models with bound states of non-scalars. Such models can be described generically at the TeV energy scale through the Chiral Lagrangian model. Chiral Perturbation Theory [6] is used to write down the Lagrangian to fourth order. With assumptions based on symmetry, we are left with two important coefficients of VBS terms, a_4 and a_5 . The value of these parameters determine the phenomenology of longitudinal VBS and represent the differences in the underlying theory.

Dynamical EWSB could also appear in extra dimensional theories without a Higgs-like particle. In this case EWSB can arise from boundary conditions at branes in warped higher dimensions [5].

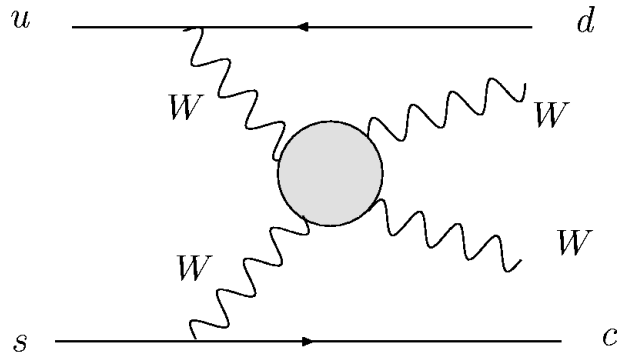


Figure 2.3: $WW \rightarrow WW$ scattering [8]

Chapter 3: Experiment

3.1 ATLAS and the LHC

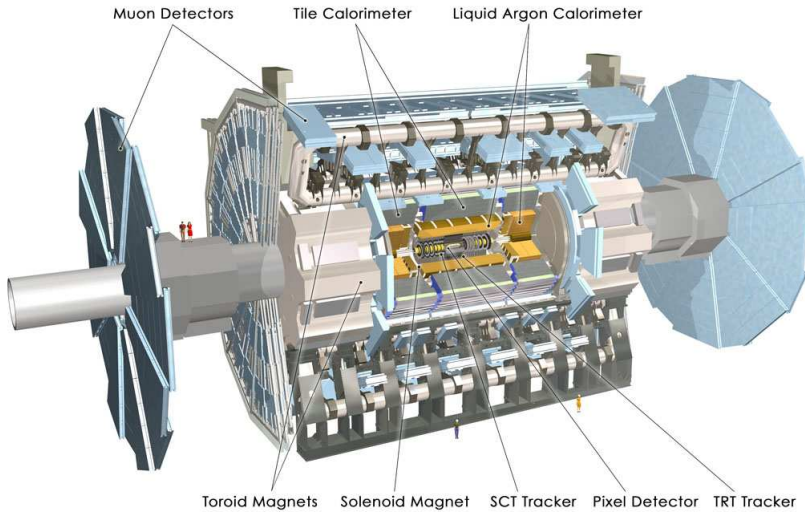


Figure 3.1: The ATLAS Detector

The LHC is a 27km circumference proton-proton collider which will provide centre of mass energies of 14 TeV and a luminosity of $10^{33} \text{ cm}^{-2} \text{ s}^{-1}$ initially up to $10^{34} \text{ cm}^{-2} \text{ s}^{-1}$ after 3 years of operation [13]. Four experiments will be constructed on the LHC, one of which is ATLAS.

Pictured in Figure 3.1, the ATLAS detector consists of the major components: an Inner Tracker, Electromagnetic and Hadronic Calorimeters and a Muon Spectrometer.

The Inner Tracker is capable of measuring the momentum and position of charged particles over 400MeV by their deflection in a 2T magnetic field. It covers as pseudorapidity range of $|\eta| < 2.5$ and consists of three subdetectors: a Transition Radiation Tracker (TRT), Semiconductor Tracker (SCT) and Pixel Detector (PD).

The electromagnetic calorimeter is lead/liquid-argon (LAr) and has an accordion geometry. It contains a barrel region of $|\eta| < 1.475$ and two endcaps at $1.375 < |\eta| < 3.2$.

The hadronic calorimeters consist of three iron scintillating-tile calorimeter. One in the barrel region $|\eta| < 1.0$ and two in the extended barrel region $0.8 < |\eta| < 1.7$. The hadronic end-caps are liquid argon and occupy $1.5 < |\eta| < 3.2$. A forward calorimeter, also liquid argon covers up to $3.1 < |\eta| < 4.9$. The large coverage of the calorimeters is vital in this PhD research due to forward jet tagging in VBS and the reconstruction of E_T^{miss} . The smaller coverage in the inner detector limits the range of calibration check for the single hadron energy scale across the calorimeters.

Finally, momentum measurements of muons will be made by tracking the deflection of muons in a magnetic field much like the Inner Detector. Few particles other than muons will pene-

trate the calorimeters and be detected in the muon chamber.

The schedule for LHC and ATLAS commissioning is given below.

- Nov-Dec 2007 - LHC collisions at 900GeV and luminosity $10^{29} \text{ cm}^{-2} \text{ s}^{-1}$.
- Mid 2008 - LHC Collisions at 14TeV with luminosity being brought up to $10^{33} \text{ cm}^{-2} \text{ s}^{-1}$.
- 2008-2011 - Luminosity increased to $10^{34} \text{ cm}^{-2} \text{ s}^{-1}$.

3.2 VBS Resonance Detection

Previous Studies have shown that detection of resonances is possible in the WZ channels [10][11]. For identification from QCD background, simulations were studied in which the W and/or Z decayed into at least one lepton. Forward jet tagging was also used for separation from background. It was shown that with 1-3 years of data taking at full luminosity a signal could be extracted for a number of models and parameters. Due to highly boosted vector bosons, an understanding of closely spaced di-jets is needed.

In the WW channel recent preliminary results have shown that data collected for 3 year at full luminosity may be enough to cover the majority of a_4 a_5 parameter space [12].

Work continues on optimisation of VBS detection, study of detector effects and ways to distinguish underlying model. As my research on this topic will not begin until mid-year, details on the specific task for this PhD project will not be given.

3.3 Calibration with Minimum Bias Events

As mentioned previously, the calibration of jets and missing energy will be very important in the reconstruction of invariant mass distributions for VBS. This is due to the large branching ratio of W and Z decays into jets and the missing energy from neutrinos in leptonic decays. Therefore, a check of the calibration for single hadron and missing energy will be performed with the use of minimum bias events.

Calibration weights are derived from test beam data and monte carlo simulations (tuned to team-beam results). This is performed at many levels of reconstruction, from the calorimeter electronics to cells and more complex cluster structures representing the energy and direction of a particle. The weights also differ for the type of physical object depositing the energy. For example, particles interacting only electromagnetic will tend to leave a larger proportion of energy in the calorimeter, while the nature of hadronic showers will lead to lost energy due (for example in nuclear break up, escaped neutrinos etc). Therefore the non-compensation of the hadronic calorimeter mean corrections must be greater for energy deposited hadronically.

The checks of calibration examined in this project will be those at the level of complex clusters and objects and will be performed in-situ with minimum bias data taken once the LHC and ATLAS are operational. It is expected that during the low luminosity 900GeV run this year $\approx 1,000,000$ events can be expected per day. At 14TeV and high luminosity, this value will

depend on trigger frequency. Such large event rates have the potential to be very powerful in checking both the single hadron energy scale and missing energy resolution. Descriptions of each are given below in more detail.

3.3.1 Single Hadron Energy Scale

Weighting is required to improve resolution and to adjust the mean reconstructed energy to the actual energy. The latter of these is what is referred to as the energy scale. Ideally the jet energy scale should be known to within $\approx 1\%$ for ATLAS. One step in this process is to check the energy scale of single hadrons. Figure 3.2 shows a scheme of the jet energy reconstruction.

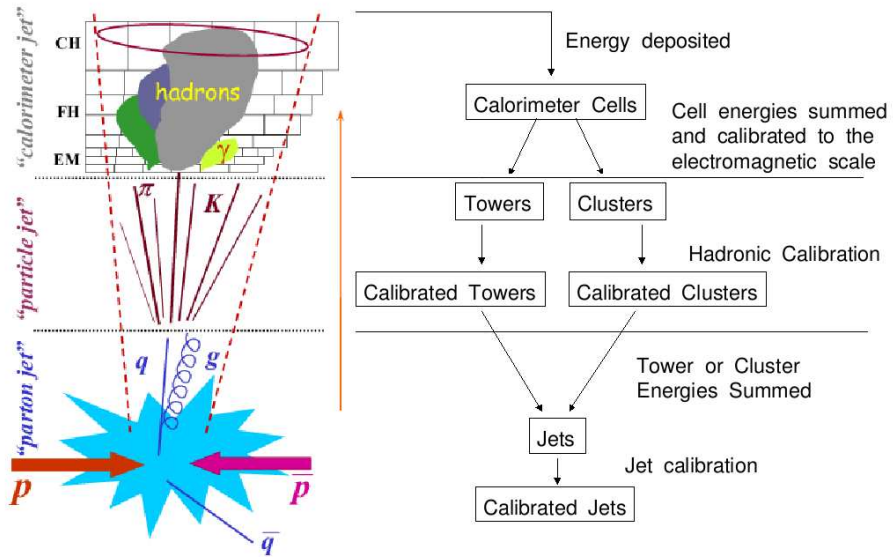


Figure 3.2: Jet Reconstruction

The objects are grouped and calibrated at each level¹:

1. Calorimeter cells are clustered to form what can loosely be associated with an individual particle.²
2. If the clusters are identified as being hadronic (through energy density and calorimeter shower depth variables), they will be calibrated to the hadronic energy scale. This accounts for the non-compensation of the ATLAS calorimeters.
3. Energy losses in dead materials are corrected for.
4. The clusters (or towers) are grouped to form jets.

¹A number of jet reconstruction algorithms perform 1-4 in a single step, bi-passing the single particle reconstruction

²In general hadronic particles may form more than one cluster when they shower. Closely spaced particles may share clusters

5. Jet calibration attempts to take into account the energy outside of the region used to group the clusters (typically a cone) and to allow for different jet fragmentation at different energies.

The final step replies on an understanding of the fragmentation of partons into hadrons. This can be simulated in monte-carlo, but relies heavily on the numerical model used as there is no experimental data on jet fragmentation at these energies. Methods to verify the jet energy scale from data can be used:

- Known mass resonance. For example $W \rightarrow jj$, $Z \rightarrow jj$.
- Momentum balance. For example $Z + j$ or $\gamma + j$.

The single hadron energy scale also needs to be checked as calibration from the test beam only tests a limited number of calorimeter modules and the setup is not identical to the full detector.

The E/p method can be used to check the single hadron energy scale across the η range of the Inner Detector. The momentum in the Inner Detector, p , will have an absolute energy scale known to within 0.5%. This can be transferred to the energy measurement in the calorimeters, E , by requiring $E/p = 1$. For this study a source of isolated charged hadrons is needed. For energies over 15 GeV, $\tau \rightarrow \nu\pi^\pm$ provides a candidate for such particles. Below 15 GeV minimum bias can be used. Further detail is given in section 4.2.1.

3.3.2 Missing Energy Resolution

The quantity E_T^{miss} is a vector (p_x^{miss}, p_y^{miss}) which represents the x and y components of the sum of energies of particles escaping detection at ATLAS. The z component can not be reconstructed due to large amounts of energy escaping in the beam pipe direction.

E_T^{miss} is calculated from:

$$E_T^{miss} + \Sigma E_T = 0$$

Where ΣE_T is the sum of transverse energies in the detector. There are various methods for reconstructing ΣE_T and all should be examined to determine which gives the best resolution and scale. The two general methods are given below.

Detector based:

$$\Sigma E_T = \Sigma p_T^{cells} + \Sigma p_T^\mu + \Sigma p_T^{jetincryostat}$$

Where Σp_T^{cells} is the transverse energy deposited in calorimeter cells up to $|\eta| < 5$, Σp_T^μ is the momentum of any muons and $\Sigma p_T^{jetincryostat}$ is an estimated correction for the jet energy lost in the cryostat gap between the electromagnetic and hadronic calorimeters.

Particle (or object) based:

$$\Sigma E_T = \Sigma p_T^{high E_T \text{ objects}(e, \gamma, \mu, \tau, jet)} + \Sigma p_T^{low E_T \text{ objects}(\pi^+, unclustered \text{ cells})}$$

Where Σp_T is the sum of particle (object) momentum in the event after reconstruction. The low momentum particles are treated differently and take into account the energy in cells not included elsewhere in the event [2].

The measurement of E_T^{miss} is an important observable because a large amount of missing energy is a signature of new physics such as the lightest supersymmetry particle and decays

of Higgs resulting in neutrinos. It is also important for the reconstruction of masses for any particles decaying in neutrinos. A large resolution in E_T^{miss} will result in broad invariant mass distributions.

Several effects will influence the resolution, scale and fake E_T^{miss} tail:

- *The Calorimeter Calibration.* This includes effects which are common to good resolution and energy scale measurements in general (not specific to E_T^{miss}): electromagnetic and hadronic cluster identification, low energy non-linearity, out of cluster energy, etc.
- *Calorimeter Coverage.* Coverage up to $|\eta| < 5$ has been shown to be required for a good E_T^{miss} value [13]. Above $|\eta| > 5$ coverage is limited and will contribute a small amount to degradation of the measurement. Additionally, inactive material losses due to leakage in crack regions between calorimeters can lead to large fake E_T^{miss} tails.
- *Noise.* Electronic and pile-up noise from minimum bias events will both contribute to this effect. It can be minimised by discounting calorimeter cells below a noise cut off of 2σ or using the 3 dimensional clustering (CaloTopoCluster) algorithm to distinguish noise from genuine energy deposits. [3].

Previous studies have shown that the resolution of each component of the vector E_T^{miss} scales as $constant \times \sqrt{E_T^{sum}}$. With the constant generally around 0.46 as shown in Figure 3.3[13]. For this project, minimum bias events will be studied to allow the low energy region of this scaling to be examined.

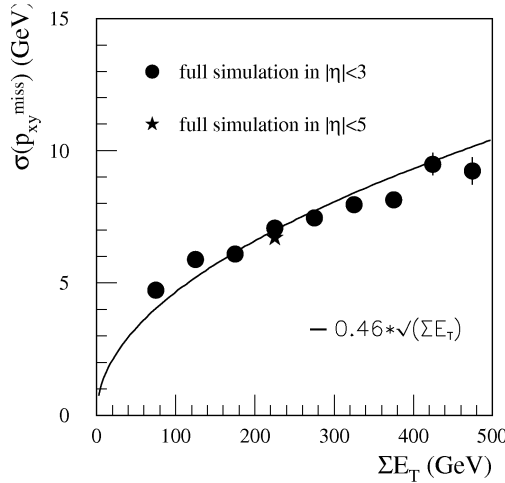


Figure 3.3: Resolution of the components of E_T^{miss} as a function of the total transverse energy for $A \rightarrow \tau\tau$ events ($m_A = 150$ GeV)

Chapter 4: Progress to Date

4.1 VBS Analysis

Work has not began on this topic apart from for the purpose of project choice.

4.2 Calibration with Minimum Bias Events

A study is about to begin on the resolution of the missing energy with minimum bias.

Work to date has focused on calibration of the single hadron energy scale. A summary of the results are given.

4.2.1 Single Hadron Energy Scale

The work on this topic has been with 50,000 Minimum Bias events which are part of the official CSC grid simulation. A full simulation, rather than a fast simulation, of the detectors response and event reconstruction was needed as energies are in the lower range of 400MeV-10GeV. This limited the number of statistics available compared to the expected real amount once data taking begins.

Minimum bias events have proven to contain many charged hadrons, with a large coverage with respect to both η and momentum (Figure 4.1). There are on average 21 tracks/event, of which $\approx 75\%$ belong to π^\pm . While this is a large source of charged hadrons the majority of these are not isolated.

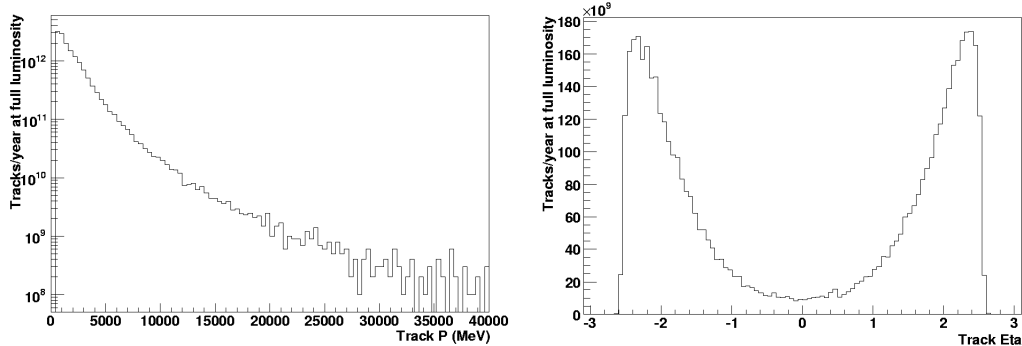


Figure 4.1: Coverage of minimum bias tracks for p and η (with $p > 2\text{GeV}$) at full luminosity (pile-up ignored)

Pions of $2.5\text{GeV} < p < 3.5\text{GeV}$ were studied and compared to 50,000 fully isolated pions in

the same energy range. E in the calorimeter was calculated by summing over the energy of CaloTopoClusters in a cone of $\Delta R = \sqrt{(\Delta\eta)^2 + (\Delta\phi)^2}$. The sample of single pions showed that over 99 % of energy was contained within a cone of size $\Delta R_{cone}=0.4$ (Figure 4.2). This was chosen as the optimal size and it minimised energy contamination from closely spaced particles but maximised energy within the cone.

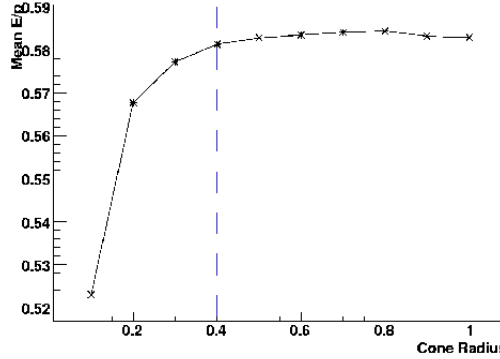


Figure 4.2: E/p as a function of cone radius ΔR_{cone}

By comparison to the single pions, a number of section cuts to identify isolated pions were determined. The cuts were kept loose for several reasons: To avoid biasing the value of E , to keep selection independent of monte-carlo simulation and to keep the statistics high enough for a comparison to $\approx 1\%$. A list of the selection cuts is given below.

1. $\Delta R_{match} < 0.05$. A matching requirement on the distance between the track (extrapolated to the 2nd layer of the electromagnetic calorimeter) and the closest cluster. At the energies examined, clusters are often not formed due to noise cut-offs in the clustering algorithm, or energy losses prior to entering the calorimeter. Additionally, tracks may be fake. Without this criteria the E/p would be biased low.
2. $\Delta R_{trackisolation} > 0.8$. Tracks must be isolated from one another. This requirement has the effect of eliminating a large proportion of the energy contamination due to charged particles. However, the efficiency of track reconstruction is between 80-95% [4]. Therefore not all contamination from charged particles is removed in this way.
3. $E_{\Delta R_{cone}=1.0} - E_{\Delta R_{cone}=0.4} < 200\text{MeV}$. The clusters must be isolated to within $\Delta R_{cone} = 1.0$. An allowance is made for low energy clusters which are potentially noise.
4. $E_{\Delta R_{cone}=0.1}/E_{\Delta R_{cone}=0.4} > 0.7$. The core 70% of energy must reside within $\Delta R_{cone} = 0.1$.
5. Number of clusters in $\Delta R_{cone} = 0.4 < 4$.
6. Number of tracks in event < 15 . For events without pile-up.

A comparison between minimum bias events and the ideal single pion sample after cuts is shown in Figure 4.4 for both the start up 900GeV centre of mass energy and 14TeV. The mean and RMS for each is shown in Tables 4.5 and 4.6. As E/p varies greatly with η , the single pion sample was weighted to have the same distribution in η as the minimum bias sample after cuts. Note that the values of E/p for this study were < 1 due to the clusters being calibrated only to the electromagnetic scale.

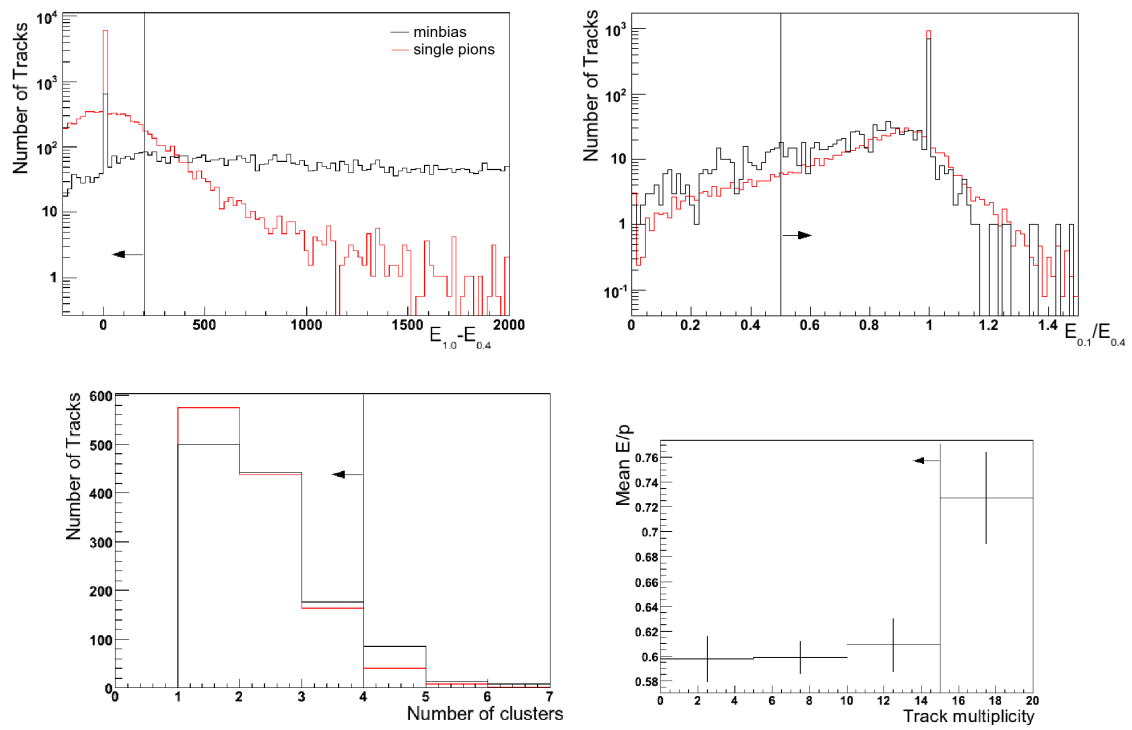


Figure 4.3: Cuts 3-6 for minimum bias and single pion samples.

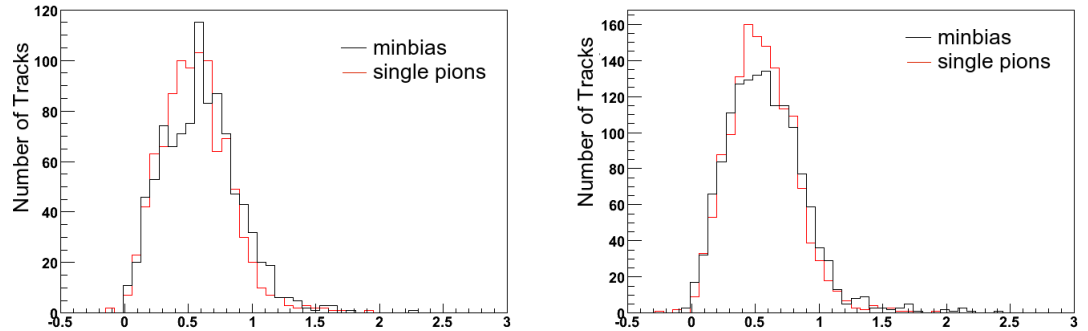


Figure 4.4: E/p distributions after select cuts for minimum bias and single pion sample for 14TeV (left) and 900GeV (right) centre of mass energies.

Sample	E/p mean	E/p RMS
Minimum Bias	0.600	0.296
Single Pions (with cuts)	0.559	0.259
Single Pions (before cuts)	0.551	0.274

Figure 4.5: Comparison of E/p for minimum bias and single pion samples. Overall bias to E/p in minimum bias events is $8\% \pm 2\%$.

Sample	E/p mean	E/p RMS
Minimum Bias	0.586	0.311
Single Pions (with cuts)	0.561	0.262
Single Pions (before cuts)	0.563	0.283

Figure 4.6: Comparison of E/p for minimum bias and single pion samples at 900GeV. Overall bias to E/p in minimum bias events is $4\% \pm 1.5\%$.

Further work is required to bring the bias below 1%. It is anticipated that a 2% bias can be lost through identification of pions from electrons. Although only $\approx 3\%$ of tracks belong to electrons, they deposit energy electromagnetically, giving an E/p close to 1. The remaining bias is due to energy contamination from close particles. Additional charged pions are a major contribution to this.

Apart from an improvement in the bias, planned future work on this topic includes:

- Study the full range of energies (400MeV to $> 20\text{GeV}$). Determine the dependence of bias on the pion energy.
- Pile-up. Overlapping minimum bias events will affect the E/p.
- Trigger. The trigger decision may affect the E/p and the amount of statistics.
- Jet Energy. E will be taken as the energy of the pion reconstructed as a jet.

Chapter 5: List of Publications and Presentations

5.1 ATLAS Internal Notes

I will contribute to the following Computer System Commissioning (CSC) Notes. These are currently being written with final versions to be completed by April. More detail of these notes, including abstracts, can be found at
<https://twiki.cern.ch/twiki/bin/view/Atlas/ReadinessNotes>

- CSC Note - JET8: Single hadron energy scale in ATLAS - section: E/p performance for low energy pions.
- CSC Note - MissingEt Overall Performance - section: Etmiss in early data, resolution in minimum bias events (with N. Kanaya, Kobe and G. Atkinson, Uni. of Melb.)

5.2 Presentations External to the University of Melbourne

Slides from the presentations below can be found at
<http://www.ph.unimelb.edu.au/~ndavidson/>

CERN Meetings:

- Geneva - JetRec Working Group Meeting - 9th Aug 2006 - Minimum Bias E/p Calibration
- Barcelona - Calorimeter Calibration Workshop - 7th Sep 2006 - Help from tracks to jet measurements (A presentation by M. Hodgkinson which included slides on E/p work)
- Geneva - JetRec Working Group Meeting - 18th Oct 2006 - Minimum Bias E/p Calibration update
- Geneva - JetRec Working Group Meeting - 24th Jan 2007 - Minimum Bias E/p Calibration update (Given by P. Lock)

Conferences:

- Brisbane - AIP Congress - 4th Dec 2006 - Hadronic In-Situ Calibration of the ATLAS Detector

- Melbourne - Texas Symposium - 11th-15th Dec 2006 - SUSY in ATLAS (Poster, with contributions from A. Phan and A. Dowler)

Chapter 6: Proposed Schedule and Timeline

6.1 Timeline to date

Year	Months	Research Task/ Significant Event	Estimated Proportion of Time
2006	March 27	PhD commencement	- 50%
2006	April - June	<ul style="list-style-type: none">- Researched potential PhD topics- Became familiar with the ATLAS software framework and analysis software. This included attendance at a one week tutorial in Tokyo, Japan (15-19 May)	<ul style="list-style-type: none">- 50%- 50%
2006	July - October	<ul style="list-style-type: none">- Studied at CERN near Geneva, Switzerland- Worked on single hadron energy scale calibration with minimum bias- Attended the ATLAS overview week, Stockholm, Sweden (10-14 July)- Attended the ATLAS calorimeter calibration workshop, near Barcelona, Spain (5-8 Sep.)	- 100%
2006	Nov - Jan	<ul style="list-style-type: none">- Worked on single hadron energy scale calibration with minimum bias- Attended the AIP congress, Brisbane (3-8 Dec.)- Attended the Texas Symposium, Melbourne (11-15 Dec.)	- 100%

6.2 Timeline of proposed research

Year	Months	Research Task/ Significant Event	Estimated proportion of time
2007	Feb - May	<ul style="list-style-type: none"> - Continue E/p work including writing CSC Note - Jet 8 - Study missing energy resolution with minimum bias data including writing CSC Note Etmiss - Begin to review theory behind VBS and mechanics for electro weak symmetry breaking beyond the standard model. 	<ul style="list-style-type: none"> - 40% - 40% - 20%
2007	June - August	<ul style="list-style-type: none"> - Continue review of theory behind VBS - Review current experimental feasibility studies with ATLAS for VBS - Begin study on VBS with ATLAS monte-calo samples 	<ul style="list-style-type: none"> - 30 % - 30% - 40 %
2007	August - Dec	<ul style="list-style-type: none"> - Return to CERN - Work on VBS studies - Attend European High Energy Particle Physics Summer School (subject to acceptance and funding), Czech Republic (19 Aug - 1 Sep) - Attend Calorimeter Calibration Workshop 	- 100%
2008	Jan-March	<ul style="list-style-type: none"> - Analyse first ATLAS data at 900GeV for calibration and publish results - Write thesis chapter on calibration results for this energy 	<ul style="list-style-type: none"> - 60% - 40%
2008	April-June	- Continue VBS analysis with monte-carlo	- 100%
2008	July-Nov	<p>Until first ATLAS data at 14TeV is taken:</p> <ul style="list-style-type: none"> - Continue VBS work - Write thesis chapter on VBS theory <p>When (if) first ATLAS data at 14TeV is taken:</p> <ul style="list-style-type: none"> - Analyse data for calibration purposes - Analyse data for detection of VBS resonances 	<ul style="list-style-type: none"> - 80% - 20% - 30% - 70%
2008	Dec - March 2009	- Write remaining research thesis chapters on VBS and calibration results for 14 TeV collisions	- 100 %
2009	March 26th	- Submission of PhD Thesis	

Bibliography

- [1] W-M Yao eta al 2006 *J. Phys. G: Nucl.Part. Phys.* 33 1 (The PDG)
- [2] N. Kanaya Sep 12-16 2006 Expected $P_{T\text{miss}}$ performance in ATLAS and CMS cHarged2006, Uppsala (Presentation)
- [3] A. Gupta June 5-9 2006 Missing E_T Reconstruction in the ATLAS Calorimeter Calor 2006, Chicago (Presentation)
- [4] D. Froidevaux and P. Sphicas 2006 General-Purpose Detectors for the Large Hadron Collider *Annu. Rev. Nucl. Part. Sci.*
- [5] C. Csaki, C. Grojean, L. Pilo and J. Terning. 2004 *Phys Rev Lett.* 92, 101802 [[hep-ph/0308038](#)]
- [6] S. Weinberg 1979 *Physica* 96A 327.
- [7] <http://en.wikipedia.org/wiki/Image:Interactions.png> Wikipedia
- [8] E. Accomando et al 2006 Isolating Vector Boson Scattering at the LHC: gauge cancellations and the Equivalent Vector Boson Approximation vs complete calculations [[hep-ph/0608019](#)]
- [9] LEP Electroweak Working Group, status of August 2005, <http://lepwwg.web.cern.ch/LEPEWWG>
- [10] G. Azuelos et al June 2006 Resonant Vector Boson Scattering at Hight Mass - Analysis of DC2 simulated data (ATLAS Internal Note)
- [11] A. Miagkov 1999 Vector boson scattering in Chiral Lagrangian model (ATLAS Internal Note)
- [12] E. Ozcan and J. Butterworth Nov 2006 Sensitivity contours for $W+W-$ (ATLAS VB Scattering CSC note meeting)
- [13] The ATLAS Collaboration 1999 ATLAS. Detector and Physics Performance Technical Design Report